Journal of Geochemical Exploration 158 (2015) 155–167

Contents lists available at ScienceDirect

Journal of Geochemical Exploration

journal homepage: www.elsevier.com/locate/jgeoexp

Computational simulation of iron ore-forming processes in the Caiyuanzi siderite ore district, Guizhou, China

Yao Liu [a,*], Tagen Dai [a,b], Shunhui Xia [c], Hailong Tian [d]

[a] Computational Geosciences Research Center, Central South University, Changsha 410083, China
[b] The Key laboratory of Chinese Education Ministry for Non-ferrous Metal Metallogenic Prediction, Central South University, Changsha 410083, China
[c] The Customer Support Center of Hunan Telecom, Changsha 410016, China
[d] Key Laboratory of Groundwater Resources and Environment, Ministry of Education, Jilin University, Changchun 130021, China

ARTICLE INFO

Article history:
Received 25 April 2015
Revised 14 July 2015
Accepted 20 July 2015
Available online 26 July 2015

Keywords:
FLAC
Caiyuanzi siderite ore district
Heat transfer
Equilibrium concentration
Hydrothermal mineralization

ABSTRACT

By means of the FISH language in the FLAC code, the coupled pore-fluid flow, heat transfer and mineralization have been simulated first with a generic model, and then with an actual geological model in the Caiyuanzi siderite ore district, Guizhou. The effect of pore-fluid pressure on the equilibrium concentration of siderite has been considered. The main purposes of this paper are: (1) to illustrate some simulation results for the possibility of hydrothermal mineralization of siderite in a sedimentary environment; (2) to get a better understanding of the processes and mechanism of siderite orebody formation in the sedimentary environment; (3) to analyze the influence of the concentration of carbon dioxide on the siderite mineralization; and (4) to compare the simulation results with the actual situation, so as to demonstrate that this simulation method is effective and feasible for understanding the mineralization mechanism of iron ore in the Caiyuanzi siderite ore district.

1. Introduction

With the significant advancements of computational science and computer technology, the computational simulation method, as a new method for dealing with a lot of complex problems in the field of mineral exploration, has attracted increasing interest of research. From the existing extensive studies carried out by Zhao et al. (1998, 2008a,b, 2009) and others (Ju et al., 2011; Lin et al., 2003, 2009; Liu et al., 2005, 2010b, 2011; Ord et al., 2002, 2008a; Xing and Makinouchi, 2008; Yan et al., 2003; Zhao, 2009, 2015), it has been well known that an ore-forming system commonly involves several processes, such as rock deformation, pore-fluid flow, heat transfer, mass transport and chemical reactions. The published papers in this research field can be briefly classified into the following categories: (1) numerical simulation and theoretical analyses of coupled heat transfer and pore fluid flow processes without considering the rock deformation (Hobbs et al., 2006, 2007; Phillips, 1991; Zhao et al., 1998, 2008b); (2) numerical simulation and theoretical analyses of convective and advective heat transfer in geological systems (Gow et al., 2002; Hobbs et al., 2000, 2004; Ord et al., 2008b, 2010; Zhao et al., 2012, 2013); (3) theoretical study of chemical dissolution and mineral precipitation instability problems (Hobbs et al., 2008, 2010a,b; Hornby et al., 2006a,b, 2008; Poulet and Regenauer-Lieb, 2015a,b; Zhao, 2014; Zhao et al., 2015a,b); and (4) application of numerical simulation to different ore-forming systems in different geological regions (Gessner et al., 2009; Schaubs and Zhao, 2002; Sorjonen-Ward and Zhang, 2002; Yang et al., 2010; Zhang et al., 2003, 2008, 2011) and to various types of geoscience problems (Alt-Epping and Zhao, 2010; Garven et al., 1993; Lei et al., 2013; Lin et al., 2006, 2008; Poulet et al., 2013; Zhao et al., 2010).

Among the above-mentioned research achievements, Zhao et al. (1998, 2008a,b, 2009) have conducted primitive and pioneering work on reactive fluid mixing and mineralization in pore-fluid saturated hydrothermal systems. In particular, Zhao et al. (2002, 2008a, 2009) proposed, for the first time, the mineralization rate concept and modern mineralization theory, which were successfully applied to the finite element simulation of mineralization patterns in hydrothermal systems, and excellent results have been obtained (Hobbs et al., 2000, 2006; Ohmoto and Lasage, 1982; Reid et al., 2012a,b; Zhao et al., 1998, 2008b). In this paper, we will add the function of Zhao's modern mineralization theory (Zhao et al., 2002, 2008a) in the FLAC code through using the FISH language, and then apply this theory to predict the mineralization patterns in the Caiyuanzi iron district.

The Caiyuanzi iron deposit is a large siderite ore deposit in Guizhou province, which has the characters of high-grade and large-scale (Lin et al., 1986). Because of both economic and scientific importance, the Caiyuanzi ore district has been widely exploited, and investigated intensively by many researchers (Lin et al., 1986; Nie, 1986). These researchers concluded that the siderite ore in the Caiyuanzi district was formed by sedimentary deformation. In recent years, other studies

* Corresponding author.
E-mail address: liuyao168@163.com (Y. Liu).

http://dx.doi.org/10.1016/j.gexplo.2015.07.012
0375-6742/

(Zhang et al., 2014) have shown that the siderite ore may be precipitated by hydrothermal transformation. This new view on the mineralization of the siderite gives us a chance to get better understanding of ore formation and mineralization in the Caiyuanzi ore district, but the preliminary research results (Yang et al., 2011) still provide some useful information about the Caiyuanzi iron deposit. We can briefly summarize the preliminary research results (Yang et al., 2011) as follows: (1) the storage situation and distribution characters of siderite resources in the Caiyuanzi iron district have been investigated; (2) the strata and the structure in the Caiyuanzi district have been determined; and (3) the siderite ore are controlled by stratum obviously. In addition, the new research results (Zhai, 2008) also give some valuable messages. They can be summarized as follows: (1) the metallogenetic resource comes from the hydrothermal fluids which are carrying the iron ion; (2) the hydrothermal intrusions was caused by the surrounding rock crack; and (3) the common way of ore forming is through the hydrothermal fluids penetrating a carbonate layer, where a chemical reaction should take place.

However, the ore-forming process in the Caiyuanzi ore district is very complex. There are still several key factors that have been ignored. For example, (1) the effects of temperature and pressure gradient on the siderite ore deposits have not been analyzed in this district; (2) the control of structures on the localization of orebodies is emphasized, but the processes of ore migration are seldom considered; (3) the research of related chemical reactions for siderite precipitation is still not deep enough; (4) many studies are restricted to the traditional methods, and the new approach of computational simulation (Liu and Dai, 2014; Zhao et al., 2009) has not been tried in the Caiyuanzi iron deposit; and (5) the influence of the concentration of carbon dioxide on the siderite mineralization has seldom been analyzed. Therefore, it is necessary to develop innovative knowledge models for understanding ore-forming processes in detail, so as to facilitate the understanding of ore formation processes in the Caiyuanzi ore district.

In this study, we use the numerical simulation method (Liu and Dai, 2014) and the modern mineralization theory (Zhao et al., 2002) to investigate the iron ore-forming mechanism of the Caiyuanzi iron deposit. The outcome of this study will not only enrich the contents of the emerging computational geoscience discipline (Hobbs et al., 2011; Ord et al., 2012, 2013a,b; Peng et al., 2008, 2011; Zhao et al., 2009), the methodology of which has been used to solve many geoscience problems (e.g., Reid et al., 2012a,b; Schmidt Mumm et al., 2010; Turcotte and Schubert, 2002; Walshe et al., 2001; Zhao, 2009, 2014; Zhao et al., 2014, 2015a, 2015b), but also give us a better understanding of the ore-formation processes in this region.

2. Geological setting

2.1. The Caiyuanzi iron district

The Caiyuanzi iron district in Guizhou province, located in the Northwest of China, is an important district of siderite deposits and has the following features: (1) the ore reserve is substantial; (2) the iron orebodies were well preserved; and (3) the iron orebodies in this district are of high-grade and large-scale, so that this district has great potential prospect for exploitation (Zhang et al., 2014). The main disputes of ore-forming genesis in this district fall into two categories: hydrothermal transformation and sedimentary deformation. Currently, most iron bodies are located in the first lithologic segment of the Dushan formation, and the local siderite is presented in the Shujiaping formation and the Longshuidong formation. The reservoir rocks are mainly composed of the Lower and the Middle Devonian carbonate, while the main ore mineral is siderite in this region. In addition, due to the excellent geographical environment and convenient traffic condition, this district has become one of the important siderite exploitation regions in China (Lin et al., 1986; Liu and Nie, 1985).

2.1.1. Strata

In the Caiyuanzi iron district, the main strata comprise the Late Silurian strata and the Devonian strata (Yan et al., 2012; Zhang et al., 2014). Among them the Middle Devonian strata and the Late Devonian strata are the main ore-bearing strata with the lithologies dominated by carbonate (Zhang et al., 2014). The sequence of the strata is shown in Table 1, where the Late Devonian Yaosuo formation and Wangchengpo formation are mainly composed of Shaly sandstone; the Middle Devonian Dushan formation with dolomite is the major metallogenic region of siderite; the main material in the Middle Devonian Dahekou formation is quartz sandstone; the Middle Devonian Longdongshui formation and the Early Devonian Shujiaping formation are dominated by muddy dolomite with a small amount of siderite deposits; the Early Devonian Danlin formation contains the quartz sandstone as the main component; and the Late Silurian Hanjiadian formation is filled by silica classic rock.

2.1.2. Structure

The fault structure is commonly developed in the Caiyuanzi field. The main structure is the NW–SE fault with seldom fold, and the width of fault crush belt is between 30 and 50 m. The rocks are mainly made up of limestone, dolomite and quartz sandstone. The rock structure of limestone is not complex. Most of them are worm-like and banded structures and located within the Middle Ordovician Dushan formation and the Early Ordovician Shujiaping formation. The dolomite, which is located within the Middle Ordovician and the Early Ordovician carbonate layer, has three main rock structures: layered structure, blocky texture and brecciated structure. The rock structure of quartz sandstone is of simple and massive texture feature, which is mainly distributed within the Middle Ordovician Dahegou formation and the Early Ordovician Danlin formation. The geological map is shown in Fig. 1.

2.1.3. Mineralization

The main ore deposit is the siderite ore in the Caiyuanzi district. There are two previous statements about the mineralization of siderite. Some researchers (Hu, 1985; Liao et al., 1980) believed that the siderite ore was formed by sedimentary deformation, because the main structure in Caiyuanzi district is the multi-layer structure, and the location of the siderite ore was controlled by the certain strata strictly. Other studies, such as the geochemical anomaly investigation (Yan et al., 2012), the enclosure parameter analysis (Zhang et al., 2014) and rock alteration research, suggested that the siderite ore could be precipitated by hydrothermal transformation.

2.2. The deposit character of the Caiyuanzi iron district

The siderite in the Caiyuanzi district is located on the south of Yangzi landmass. This district is characterized by complex geological structures, developed multi-layer strata, strong fault actions, predominant metallogenic condition and rich siderite ore resources. Thus, it formed a centralized zone of mineralization and also constituted one of the important large siderite ore deposits. This is why the geological research on this deposit is of great significance (Guizhou Bureau and of Geology and Mineral Resources, 1987).

The major siderite ore was located in the Middle Devonian Dushan formation (D_2d^1) carbonate layer, and the fewer deposit was hosted in the Middle Devonian Longdongshui formation (D_2l) and Shujiaping formation (D_2s) carbonate layers. The distributions of the four larger orebodies are from northwest to southeast, which belong to the completely-concealed ore deposit. The dip angles of the deposit are about 5–35°. The ore deposit is extended about 1000–1600 m in the NW direction, while the width of the ore deposit is between 150 m and 300 m. There is little impurity in the ore samples, so that the siderite content can reach about 90%. The mineralization temperature measured from the 10 siderite ore samples is about 195–260 °C, with an average mineralization temperature of 217 °C.

Table 1
Stratigraphy and thickness of the strata in the Caiyuanzi siderite ore district (see Zhang et al., 2014).

Period	Epoch	Series	Lithostratigraphic unit	Member	Stratum code	Thickness (m)
Cenozoic	Quaternary				Q	>20
Late Paleozoic	Devonian	Late	Yaosuo formation		D_3y	70–130
			Wangchengpo formation		D_3w	90–130
		Middle	Dushan formation	Jiwozhai	$D2d^3$	100–130
			Dushan formation	Songjiaqiao	$D2d^2$	20–50
			Dushan formation	Jipao	$D2d^1$	120–200
			Dahekou formation		D2*dh*	0–140
			Longdongshui formation		D2*l*	20–100
		Early	Shujiaping formation		D1*s*	0–50
			Danlin formation		D1*d*	0–100
Early Paleozoic	Silurian	Late	Hanjiadian formation		S1*h*	170–315

3. Computational methodology

3.1. Brief introduction of the FLAC software

The Fast Lagrangian Analysis of Continua (FLAC) code (Itasca Consulting Group, 2002) is used to simulate the mineralization process of the Caiyuanzi iron deposit. FLAC is a two dimensional explicit finite difference code, which has been widely used for solving complex geoscience problems involving rock deformation, pore-fluid flow, heat transfer and the coupling between them (Forrest and Eunhye, 2013; Hakami, 2001; Liu et al., 2011).

Compared with the finite element models, the explicit finite difference models have the following advantages: (1) it can be used to calculate nonlinear constitutive relationships directly, without excessive memory requirements. (2) A large number of grid cells may be modeled with a modest memory requirement, because there is no global stiffness matrix that needs to be inverted during each time-step. (3) FLAC is robust in the sense that it can handle any constitutive model with no adjustment to the solution algorithms and techniques for different constitutive models. The open programming design option makes it easy for the users to use their own programming techniques within the framework of the FLAC code through the FISH language. Large-

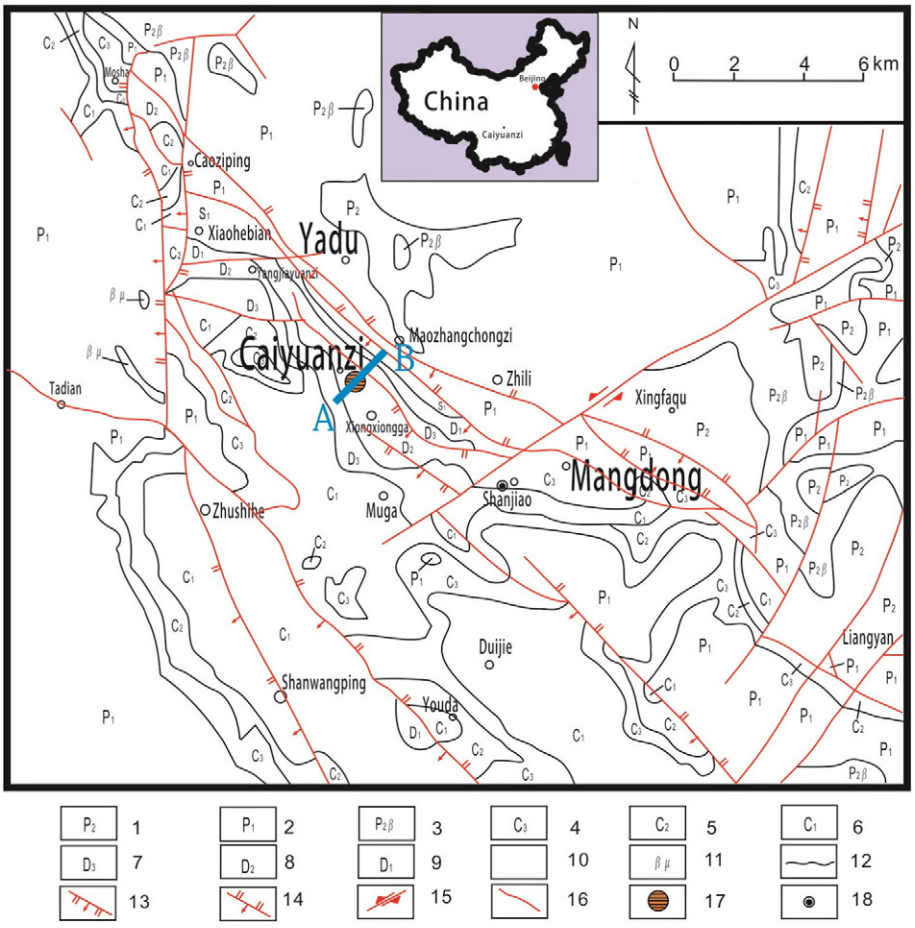

Fig. 1. Geological map of the siderite ore deposits in the part of the Hezhang county, showing the location of the Caiyuanzi iron deposit. 1. Upper Permian; 2. Lower Permian; 3. Emeishan basalt; 4. Upper Carboniferous; 5. Middle Carboniferous; 6. Lower Carboniferous; 7. Upper Devonian; 8. Middle Devonian; 9. Lower Devonian; 10. Lower Silurian; 11. diabase; 12. Geological boundaries; 13. normal fault; 14. thrust fault; 15. Strike-slip fault; 16. Unknown fault; 17. Siderite ore deposit; 18. mineralized spot.
Modified from Zhang et al. (2014).

scale complex problems can be simulated using the FLAC code, and computational time would not increase significantly for highly nonlinear problems (Cundall and Board, 1988; Strayer et al., 2001; Tiziana et al., 2013; Xiao et al., 2005; Xie et al., 1999).

3.2. Governing equations

As mentioned previously, the hydrothermal transformation of the siderite ore should be caused by a thermal process, which is controlled by the temperature gradient in porous rocks (Zhao et al., 1998, 2008a, 2015a,b). As the hydrothermal fluid passed through the carbonate layer, a strongly chemical reaction was presented, so that the siderite ore was formed. Since the mineralization rate, which is presented by Zhao et al. (2002, 2008a), has been successfully used to simulate the precipitation of the magnetite in the Fushan iron deposit (Liu and Dai, 2014), it can be further extended to explain the iron ore-forming process, in which the siderite ore is formed by hydrothermal transformation in the Caiyuanzi iron district. The governing equations used for simulating the iron ore-forming process of the Caiyuanzi ore deposit in the FLAC models can be briefly described as follows:

$$\upsilon_x^f = -\frac{k_x \lambda(s)}{\mu}\frac{\partial P}{\partial x} \tag{1}$$

$$\upsilon_y^f = -\frac{k_y \lambda(s)}{\mu}\left(\frac{\partial P}{\partial y} - \rho_f g\right) \tag{2}$$

$$q_x^T = -\left(\phi\xi^f + (1-\phi)\xi^s\right)\frac{\partial T}{\partial x} \tag{3}$$

$$q_y^T = -\left(\phi\xi^f + (1-\phi)\xi^s\right)\frac{\partial T}{\partial y} \tag{4}$$

$$\rho_f = \rho_0[1-\beta(T-T_0)] \tag{5}$$

where υ_x^f and υ_y^f are the Darcy velocities of fluid flow in the x and y directions, respectively; P is the pressure of the pore-fluid; k_x and k_y are the mobility coefficients (FLAC's permeability) in the x and y directions, respectively; $\lambda(s)$ is a function of saturation s; μ is the dynamic viscosity of the pore-fluid; g is the component of gravitational acceleration in the y direction; ρ_f is the density of the pore-fluid; q_x^T and q_y^T are the thermal fluxes in the x and y directions, respectively; ξ^f and ξ^s are the thermal conductivity coefficients of the pore-fluid and solid matrix, respectively; T is the temperature; and ϕ is the porosity (Liu et al., 2010a; Zhao et al., 2008a). ρ_0 is the reference density of the pore-fluid; β is the volumetric thermal expansion coefficient; and T and T_0 are the temperature and reference temperature of the pore-fluid and surrounding medium, respectively.

Eqs. (1) and (2) are the Darcy law describing pore-fluid flow in the x and y directions, respectively. Eqs. (3) and (4) are the Fourier law describing heat transfer in the x and y directions, respectively; while Eq. (5) is the relationship between temperature and the pore-fluid density. The governing equations describe the conservation of mass, energy and momentum. The coupled thermal–hydrological constitutive relations can be found in the literature (Liu et al., 2010a; Xie et al., 1999; Zhao et al., 1998, 2008a, 2009).

In the previous numerical simulation of the magnetite mineralization in the Fushan iron deposit (Liu and Dai, 2014), the influence between the coupling of porosity and the volumetric change rate has

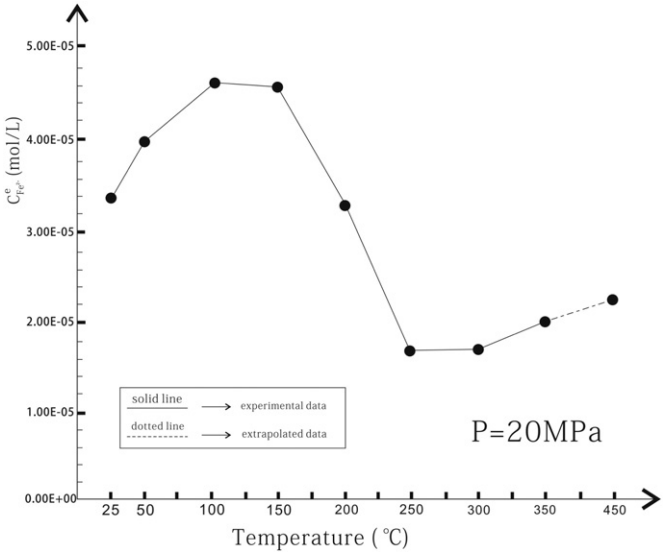

Fig. 2. Variations of iron ion (Fe^{2+}) equilibrium concentration with temperature (in the NaCl buffer). The experimental data are provided by the TOUGHREACT code (Xu et al., 2004).

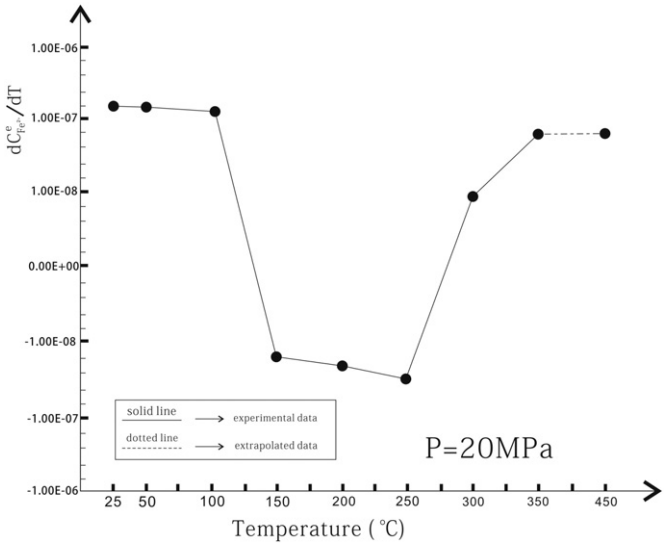

Fig. 3. Variations of the differentiation of iron ion (Fe^{2+}) equilibrium concentration with temperature (in the NaCl buffer). The experimental data are provided by the TOUGHREACT code (Xu et al., 2004).

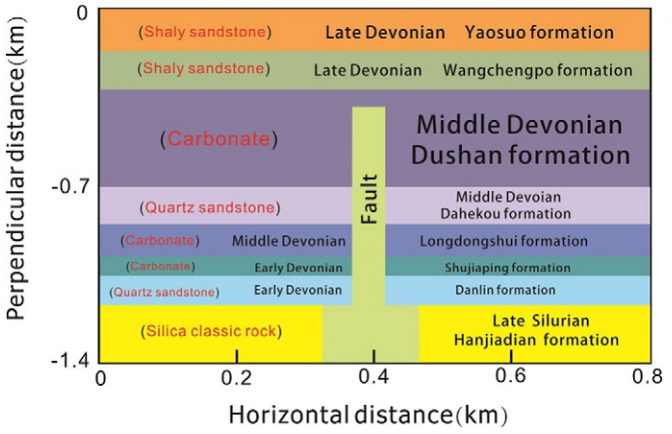

Fig. 4. The generic model of the Caiyuanzi iron deposit (the red text indicates the main rock types).

Table 2
Rock material parameters assigned for the generic model. The data are obtained from the previous studies (Cai et al., 2002; Liu and Dai, 2014; Ju et al., 2011).

Rock types	Density (kg/m^3)	Specific heat capacity (J/kg·K)	Linear thermal expansion coefficient (10^{-6}/K)	Conductivity (W/m·K)	Fluid volumetric thermal expansion (10^{-6}/K)	Grain volumetric thermal expansion (10^{-6}/K)	Permeability (m^2)	Porosity (%)
Shaly sandstone	2460	660	6.60	2.2	620	28.1	1.00×10^{-14}	20
Carbonate	2580	790	8.40	2.4	720	31.9	2.00×10^{-12}	25
Quartz sandstone	2530	710	10.80	2.0	540	25.4	1.00×10^{-14}	18
Silica classic rock	2480	730	9.60	2.2	640	29.6	2.00×10^{-14}	20
Fault zone	2400	2200	13.90	2.0	820	41.7	1.00×10^{-10}	30

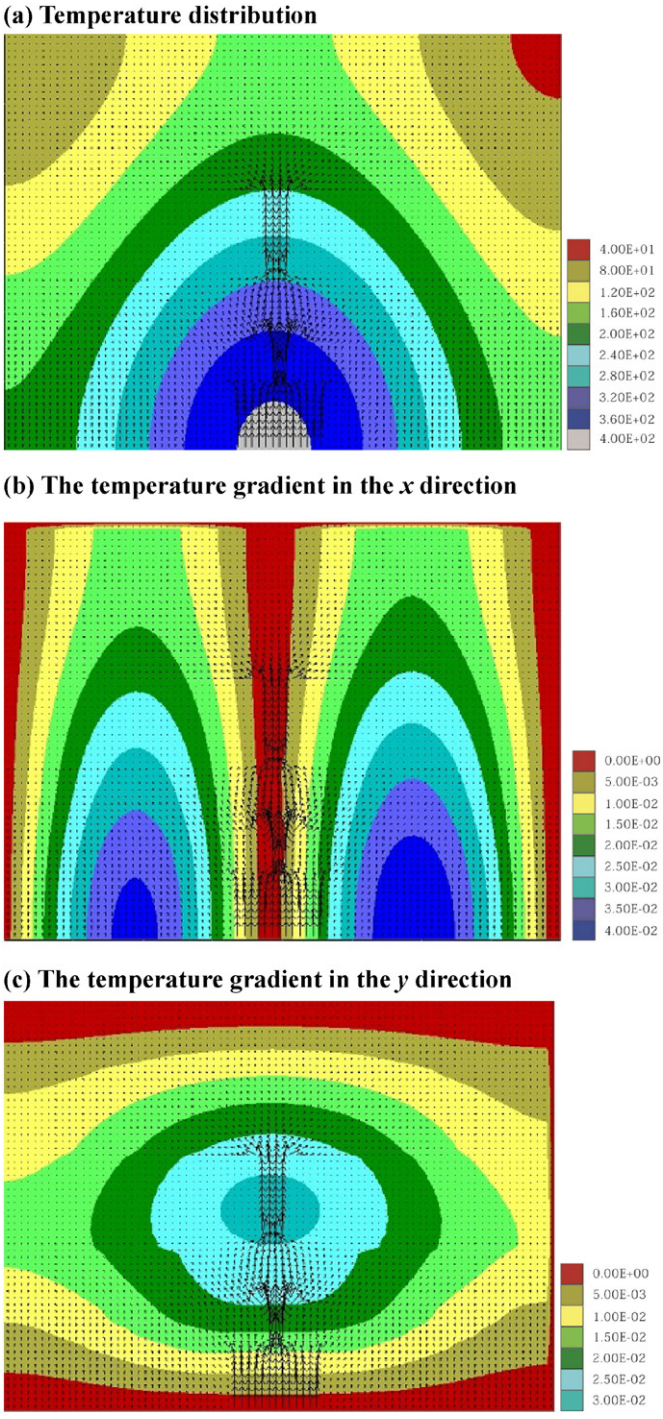

Fig. 5. Distributions of temperature and its gradients: (a) temperature distribution; (b) the temperature gradient in the *x* direction and (c) the temperature gradient in the *y* direction.

been neglected. This means that when the two dimensional FLAC program is used, the porosity is assumed to be constant, which cannot reflect the realistic situation accurately. The relationship between porosity and the volumetric change rate can be represented by the following equation (Ju, 2011):

$$n = 1 - \frac{V_0}{V}(1 - n_0) = 1 - e_V(1 - n_0) \tag{6}$$

where V_0 is the initial volume of the material; V is the total volume of the material; e_V is the volumetric change rate; n is the porosity of the material; n_0 is the initial porosity of the material. Under the large deformation condition, e_V can be approximated as (Zhao et al., 2008a, 2009):

$$e_V = \frac{2(V - V_0)}{V + V_0}. \tag{7}$$

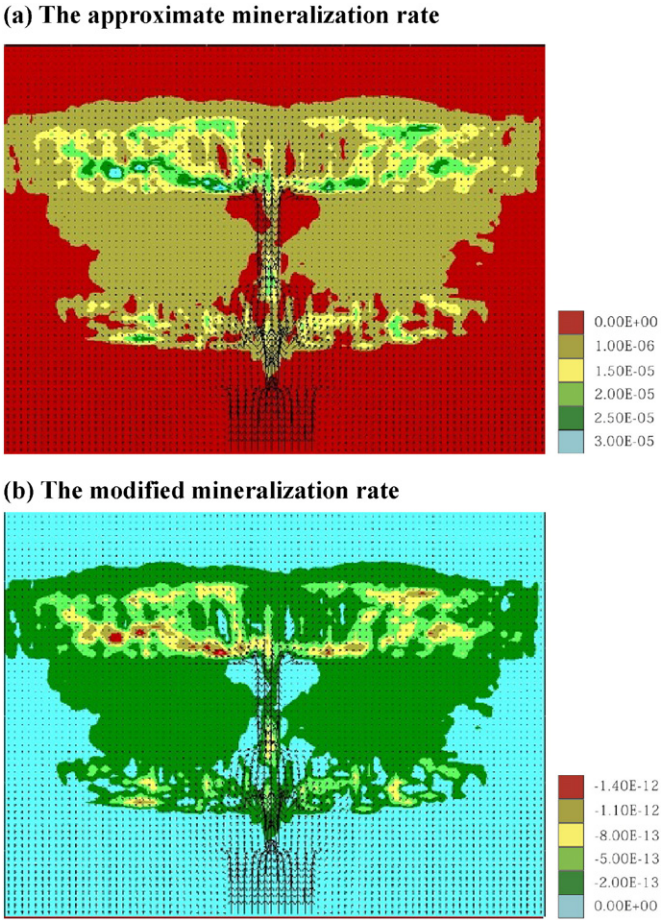

Fig. 6. Distributions of the approximate and modified mineralization rates with only considering the effect of temperature: (a) the approximate mineralization rate and (b) the modified mineralization rate.

By substituting Eq. (7) into Eq. (6), we can get:

$$n = 1 - \frac{2(V - V_0)}{V + V_0}(1 - n_0). \quad (8)$$

3.3. The concept of the mineralization rate

The mineralization rate of a mineral, which was proposed by Zhao et al. (2002, 2008a), is defined as the variation in the mineral weight per unit volume rock at per unit time during mineralization. Using this definition, the positive value of the mineralization rate of iron ore means the dissolution of iron ore in the hydrothermal system, while the negative value of the mineralization rate means the precipitation of iron ore in the hydrothermal system (Zhao et al., 2002, 2008a). The mathematical formula of the mineralization rate can be deduced from the mass conservation law as follows (Zhao et al., 2002, 2008a):

$$u_j C^e_{k,j} = \left(D^e_{ij} C^e_{k,j}\right) + \phi R_k \quad (k = 1, 2, \ldots, M) \quad (9)$$

where u_j is the velocity component in the x_j direction; C^e_k is the equilibrium concentration of mineral k, R_k is the source/sink term; M is the total number of the minerals to be considered in the ore-forming system; ϕ is the porosity of the porous rock; and D^e_{ij} is the second-order diffusivity tensor of the porous rock. For mineralization problems, the diffusion term on the right-hand side of Eq. (9) is usually much smaller than the advection term. Thus, Eq. (9) can be approximately expressed as:

$$MR_k = u_j C^e_{k,j} = \phi R_k \quad (10)$$

where MR_k is the mineralization rate of mineral k.

In general, the equilibrium concentration of a mineral is a function of temperature, pressure and other relevant minerals as follows:

$$C^e_k = f(T, P, C_1, C_2, \ldots, C_N) \quad (11)$$

where T is temperature; P is the pore-fluid pressure; C^e_k is the equilibrium concentration of mineral k; C_r $(r = 1, 2, \ldots, N)$ is the concentration of mineral; and N is the number of the relevant minerals/species to determine the equilibrium concentration of mineral/species k in the chemical reaction. According to the chain rule, substituting Eq. (11) into Eq. (10) yields the following equation (Zhao et al., 2002, 2008a):

$$MR_k = \frac{\partial C^e_k}{\partial T}(u_j T_j) + \frac{\partial C^e_k}{\partial T}(u_j P_j) + \sum_{r=1}^{n} \frac{\partial C^e_k}{\partial C_r}(u_j C_{r,j}) \quad (12)$$

where T is temperature; P is the pore-fluid pressure; C^e_k is the equilibrium concentration of mineral k; u_j is the velocity component in the x_j direction; C_r $(r = 1, 2, \ldots, N)$ is the concentration of mineral r; and N is the number of the relevant minerals/species to determine the equilibrium concentration of mineral/species k in the chemical reaction.

3.4. The equilibrium concentration of iron ion (Fe^{2+}) in siderite

According to a previous study (Hu, 1985; Liao et al., 1980), the Caiyuanzi iron deposit is located in the Late Devonian carbonate layer and the Middle Devonian carbonate layer. The main orebody is siderite in this region. Some researchers (Liao et al., 1980) believed that the

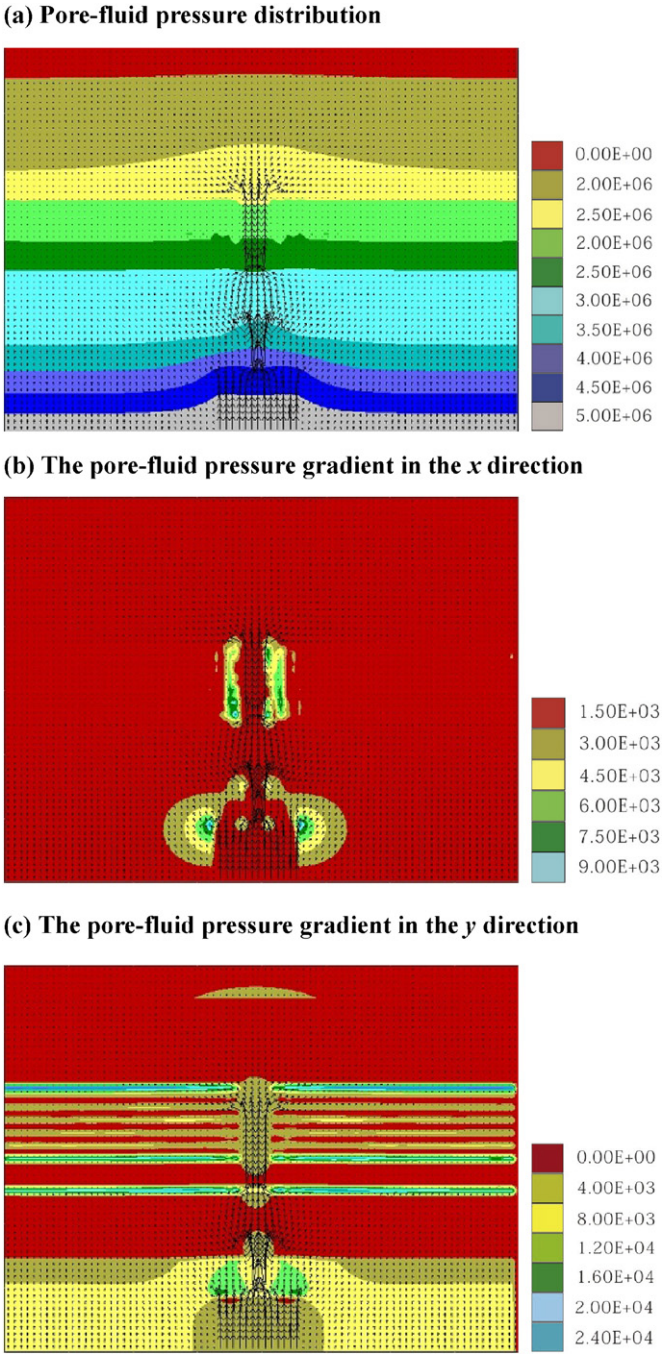

Fig. 7. Distributions of pore-fluid pressure and its gradients: (a) pore-fluid pressure distribution; (b) the pore-fluid pressure gradient in the x direction and (c) the pore-fluid pressure gradient in the y direction.

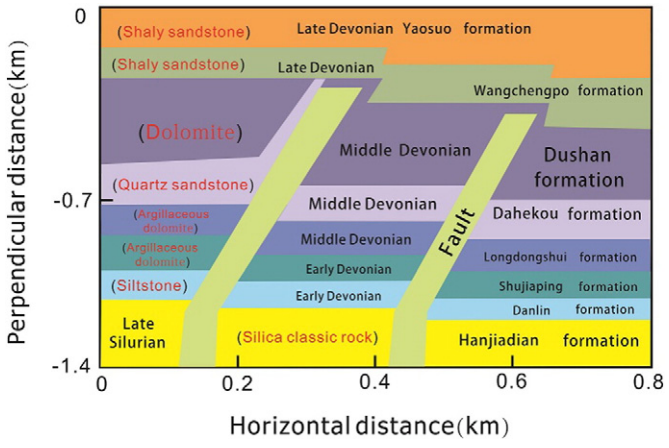

Fig. 8. The actual model of the iron deposit in the Caiyuanzi mine.

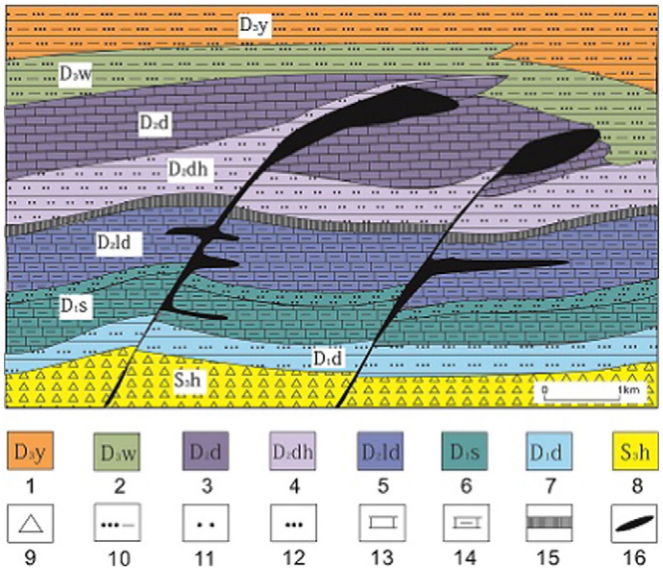

Fig. 9. The cross-section of the iron deposit in the Caiyuanzi mine: 1. the Late Devonian Yaosuo formation; 2. the Late Devonian Wangchengpo formation; 3. the Middle Devonian Dushan formation; 4. the Middle Devonian Dahekou formation; 5. the Middle Devonian Longdongshui formation; 6. the Early Devonian Shujiaping formation; 7. the Early Devonian Danlin formation; 8. the Late Silurian Hanjiadian formation; 9. silica classic rock; 10. shaly sandstone; 11. quartz sandstone; 12. siltstone; 13. dolomite; 14. argillaceous dolomite; 15. sedimentary iron ore; and 16. siderite ore deposits.

siderite ore was deposited in the carbonate layer, while other studies (Zhang et al., 2014) showed that the hydrothermal transformation is the main factor to cause mineralization. When the hydrothermal fluid contact an abundant carbonate, strong chemical reaction can take place, which is in favor of the siderite precipitation.

Since the equilibrium concentration of a mineral is strongly dependent on the local temperature, the temperature variation in a hydrothermal system may provide a favorite environment for the mineralization to take place.

For the mixing of reactive carbonate fluids, the corresponding chemical formula can be expressed, in an ionic form, as

$$FeCO_3 \overset{w}{\Longleftrightarrow} Fe^{2+} + CO_3^{-2} \tag{13}$$

where w is the overall reaction rate constant, which is strongly dependent on temperature, from the thermodynamic point of view.

The previous study (Zhang et al., 2014) shows that siderite could be easily precipitated when the pH value of the solution is 7. Because the pH value of NaCl aqueous solution almost equals to 7, it can be used as a buffer for siderite mineralization. Since the equilibrium concentration of iron ion (Fe^{2+}) in siderite has been directly calculated by the TOUGHREACT code (Xu et al., 2004) between 25 °C and 400 °C in the NaCl solution that comprises of siderite, calcium carbonate and sodium chloride, it can be used in this study for analyzing the precipitation pattern of siderite. For a NaCl buffer, the equilibrium concentration of iron ion (Fe^{2+}) in siderite at temperatures between 25 °C and 400 °C can be expressed in a piecewise manner as

$$\begin{aligned}
\log C^e_{Fe} &= 0.002499T - 4.5229 \ (25\ ^\circ C \le T < 50\ ^\circ C)\\
\log C^e_{Fe} &= 0.001564T - 4.5543 \ (50\ ^\circ C \le T < 100\ ^\circ C)\\
log C^e_{Fe} &= -0.000181T - 4.3198 \ (100\ ^\circ C \le T < 150\ ^\circ C)\\
\log C^e_{Fe} &= -0.00176T - 4.3288 \ (150\ ^\circ C \le T < 200\ ^\circ C)\\
\log C^e_{Fe} &= -0.007101T - 4.4168 \ (200\ ^\circ C \le T < 250\ ^\circ C)\\
\log C^e_{Fe} &= 0.000026T - 4.7721 \ (250\ ^\circ C \le T < 300\ ^\circ C)\\
\log C^e_{Fe} &= 0.002223T - 4.7708 \ (300\ ^\circ C \le T < 350\ ^\circ C)\\
log C^e_{Fe} &= 0.000426T - 4.7708 \ (350\ ^\circ C \le T < 400\ ^\circ C)
\end{aligned} \tag{14}$$

where C^e_{Fe} is the equilibrium concentration of iron ion (Fe^{2+}). Note that the results of the equilibrium concentration of iron ion (Fe^{2+}) at temperatures between 350 °C and 400 °C are the extrapolated data.

Fig. 2 shows the variation of iron ion (Fe^{2+}) equilibrium concentration with temperature under the NaCl buffer condition, while Fig. 3 shows the variation of the differentiation of iron ion (Fe^{2+}) equilibrium concentration with temperature under the NaCl buffer condition. The solid line is the experimental data, while the dotted line is the extrapolated data.

Based on Figs. 2 and 3, the experimental data of iron ion (Fe^{2+}) equilibrium concentration, which was obtained under the condition of the concentration of carbonate (CO_3^{2-}), is not a constant number. With an increase in the concentration of iron ion (Fe^{2+}), the equilibrium concentration of carbonate (CO_3^{2-}) is also increased. From using the TOUGHREACT-calculated equilibrium concentration of iron ion (Fe^{2+}) and carbonate (CO_3^{2-}) at different temperatures and pressures, it is obvious that the equilibrium concentration of iron ion (Fe^{2+}) and carbonate (CO_3^{2-}) is controlled by temperature and affected little by the pressure.

3.5. Computational model of the problem

A conceptual 2D model (Fig. 4) is established for the Caiyuanzi iron deposit based on the cross section along line AB in Fig. 1. A set of assumptions are made to reflect the subsurface geological conditions of the Caiyuanzi ore deposit and other features that are relevant to pore-fluid flow in this district.

In this paper, three examples are considered, which represent an 800 m long and a 1.4 km deep cross-section. The initial hot pore-fluid in the fault zone is 400 °C. The driving force of pore fluid flow is the heat anomaly. These chosen conditions are based on the following considerations.

As shown in Table 1, the existing study (Zhang et al., 2014) showed that the range of the ore-forming pressure is about 4–40 MPa. The particular distance can be calculated by the thickness of the stratum with considering the distance of fluid flow. We can assume that the deep of the model is 1.4 km. The horizontal dimension of the model is 800 m, which is similar to the length of line AB in Fig. 1. As mentioned

Table 3
Rock material parameters assigned for the actual model (Cai et al., 2002; Liu and Dai, 2014; Ju et al., 2011).

Rock types	Density (kg/m^3)	Specific heat capacity (J/kg·K)	Linear thermal expansion coefficient (10^{-6}/K)	Conductivity (W/m·K)	Fluid volumetric thermal expansion (10^{-6}/K)	Grain volumetric thermal expansion (10^{-6}/K)	Permeability (m^2)	Porosity (%)
Shaly sandstone	2460	660	6.60	2.2	620	28.1	1.00×10^{-14}	20
Dolomite	2580	790	8.40	2.4	720	31.9	2.00×10^{-11}	25
Quartz sandstone	2530	710	10.80	2.0	540	25.4	1.00×10^{-14}	18
Siltstone	2480	670	6.80	2.3	630	29.2	1.00×10^{-14}	21
Silica classic rock	2480	730	9.60	2.2	640	29.6	2.00×10^{-14}	20
Argillaceous dolomite	2520	740	8.1	2.3	690	30.6	2.00×10^{-11}	24
Fault zone	2400	2200	13.90	2.0	820	41.7	1.00×10^{-10}	30

previously, the mineralization temperature of the iron ore is about 195–260 °C, with an average mineralization temperature of 217 °C. Since the highest temperature used for the TOUGHREACT calculation in the experimental data of the equilibrium concentration of iron ion (Fe^{2+}) is about 350 °C, the equilibrium concentration of iron ion (Fe^{2+}) at temperatures between 350 °C and 400 °C are the extrapolated data. The initial temperature of the intrusion is set at 400 °C, because the initial temperature of the intrusion in the experiments must be a little higher than the highest temperature of ore-forming fluids (Liu et al., 2011). Thus, 400 °C is an acceptable initial temperature for the intrusion in the following numerical simulations. The driving force of pore fluid flow is the heat anomaly (Liu and Dai, 2014).

The 2D model consists of 4800 four-node grid cells. As shown in Fig. 4, the main strata in the Caiyuanzi iron ore district are divided into eight layers, namely the Late Devonian Yaosuo formation (shaly-sandstone layer), the Late Devonian Wangchengpo formation (shaly-sandstone layer), the Middle Devonian Dushan formation (carbonate layer), the Middle Devonian Dahekou formation (quartz-sandstone layer), the Middle Devonian Longdongshui formation (carbonate layer), the Early Devonian Shujiaping formation (carbonate layer), the Early Devonian Danlin formation (quartz-sandstone layer) and the Late Silurian Hanjiadian formation (silica classic rock layer) from the top to the bottom of the model. For the sake of general consideration, the fault zone in the generic model is assumed to be located between the up and middle of the Middle Devonian Dushan formation stratum. The depth of the fault zone is also assumed to be 1.0 km. Because most iron deposits are hosted in the Middle Devonian Dushan formation carbonate layer, it implies that abundant pore fluids had contacted with the carbonate layer, and the fault zone extended to the Middle Devonian Dushan formation carbonate layer, so that the depth of fault zone was determined based on this recognition. Due to the limitation of the computer code, our numerical experiments cannot simulate the coupled mechano-thermo-hydrological process in the current computational model, but can simulate the coupled heat transfer and pore-fluid flow with considering the mineralization rate, so that in our FLAC models, the rock deformation of the intrusion was neglected. The relevant rock material parameters in Table 2 are used in the numerical simulation.

Fig. 5 shows the distributions of the temperature, the first-order partial derivative of the temperature with respect to the x and y directions in the generic model. As mentioned by Zhao et al. (2008a, 2009), the localization of temperature can provide appropriate conditions for the orebody formation in some regions of the hydrothermal system. From the mineralization rate theory, the place where the more change of temperature and the faster velocity of pore-fluid flow is more favorable to form orebodies (Zhao et al., 2002, 2008a). Since the first-order partial derivative of temperature with respect to the x and y directions represents the temperature gradients in the x and y directions, we can use them to roughly estimate the favorable locations to form the orebodies in the hydrothermal system.

Fig. 6 shows the distributions of the approximate mineralization rate (which is equal to the scalar product of the pore-fluid velocity and temperature gradient (Zhao et al., 2002, 2008a)) and the modified mineralization rate (which is equal to the product of the approximate mineralization rate and the equilibrium concentration differentiation with respect to temperature (Zhao et al., 2008a)) of the iron ore in the generic model. Since the negative value of the mineralization rate of a mineral reflects the precipitation of the mineral and the positive value of the mineralization rate reflects the dissolution of the mineral, the precipitation regions of iron are clearly shown in the generic model. As can be seen from these modeling results, most precipitation of iron is distributed in the Middle Devonian Longdongshui formation carbonate layer and the Early Devonian Shujiaping formation carbonate layer. As observed in the Caiyuanzi iron district, mainly iron deposits are hosted in the Middle Devonian Dushan formation carbonate layer. This significant difference indicates that geological settings have a dramatic effect on the mineralization patterns of iron ore. Since the pressure dependence of solubility is typically weak and usually neglected in the chemical reaction of magnetite (Pauling, 1988), the change of pressure has not been coded in the program (Liu and Dai, 2014). Because the experimental data of the equilibrium concentration of iron ion, which are provided by the TOUGHREACT code, showed that the pressure has also little impact to the equilibrium of the chemical reaction of siderite, the influence of pressure on the siderite precipitation has not been considered in the related numerical simulations.

Fig. 7 shows the distributions of the pore-fluid pressure, the pore-pressure gradients in the x and y directions within the generic model. Eq. (12) shows that the mineralization rate is dependent on many factors. In the previous section, the variation of the temperature gradient has been considered in the computational simulation, and the role of

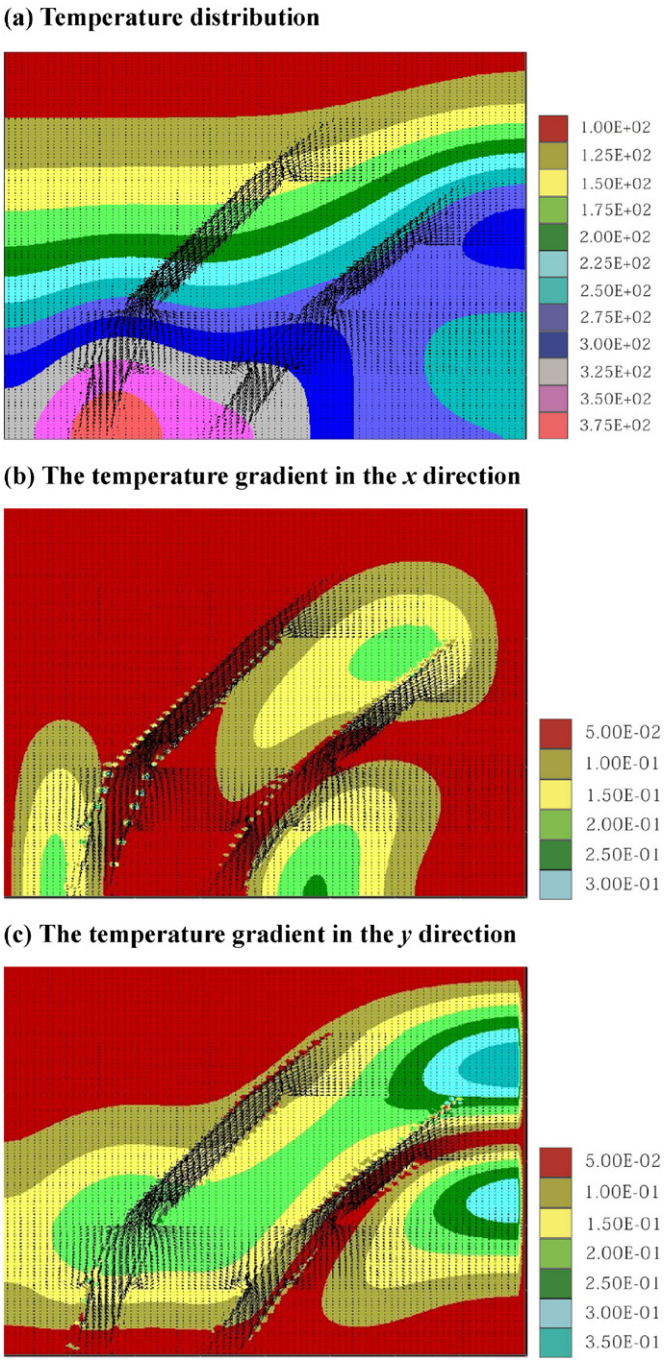

Fig. 10. Distributions of temperature and its gradients: (a) temperature distribution; (b) the temperature gradient in the x direction and (c) the temperature gradient in the y direction.

pore-fluid pressure in the mineralization rate is similar to that of temperature. From the experimental data of the solubility of siderite, which are provided by the TOUGHREACT code, the distributions of pore-fluid pressure and its gradients has little affect on the mineralization pattern, so that they can be neglected in the computation. However, the distributions of pore-fluid pressure and its gradients have been given here for the reference in the future research, when some new data of chemical reactions are obtained in the Caiyuanzi ore district. As shown in Fig. 7, the significant change of the pore-fluid pressure gradient in the *x* direction takes place around the fault zone, while the significant change of the pore-fluid pressure gradient in the *x* direction takes place on the verge of the Middle Devonian Dushan formation carbonate stratum, the Middle Devonian Longdongshui formation carbonate stratum and the Early Devonian Shujiaping formation carbonate stratum.

The numerical model of the second example is constructed by considering one of the geological section maps of the Caiyuanzi iron deposit, as shown in Fig. 8. This model, which is called the actual model, is filled with more complex rocks and comprised of 4800 four-node grid cells. The rocks considered in this model are the shaly sandstone, dolomite, quartz sandstone, argillaceous dolomite, silt stone and silica classic rock. In Fig. 8, there are two parallel fault zones, the dip angles of which are both 45° to the east. The fault distributions in the model are based on the geological cross-section map in Fig. 9. To consider the rock erosion situation during the mineralization and present day, the space between the top boundary of the model and the surface of the profile map is filled with the corresponding rock. The relevant rock material parameters listed in Table 3 are used in the numerical modeling, also without considering the rock deformation.

Fig. 10a shows the distributions of temperature, while Fig. 10b and c shows the distributions of temperature gradient in the *x* and *y* directions of the actual model, respectively. The results in Fig. 5 show that the distribution of temperature is symmetrical in the fault trend direction completely. On each side of the fault, the temperature gradient in the *x* direction is exactly the same. Fig. 10 shows that the location of the two parallel faults are near the west of the bottom, and the attitude of the fault zone has a dip angle of 45° to the east, so that the distribution of temperature is diffused along the faults trend. The temperature gradient in the *x* and *y* directions shows that the temperature has changed a lot in the regions which are favorable for the siderite precipitation. This indicates that both the position and intrusion directions of the fault zone can have a significant influence on the temperature localization in a hydrothermal system.

Fig. 11 shows the distributions of the approximate and modified mineralization rates of siderite ore in the actual model of the Caiyuanzi iron deposit. In this figure, Fig. 11a shows the approximate mineralization rate of siderite, while Fig. 11b shows the modified mineralization rate of siderite.

Fig. 12 shows the distributions of the pore-fluid pressure and its gradients in the *x* and *y* directions within the actual model of the Caiyuanzi iron deposit. It is obvious that the modeling results in this case are similar to those shown in Fig. 5, but the corresponding variation regions are relatively smaller. Note that since the pore-fluid pressure distribution is affected by the rock mechanical properties, the distributions of permeability and porosity play a major role in the formation of the Caiyuanzi iron deposit.

The third example is to use the refined grids of the second model. In this case, the numerical model is composed of 19,200 four-node grid cells, which are four times the number of grid cells used in the second example. The geological environment and the relevant parameters are exactly the same as those used in the second example. Fig. 13 shows the distributions of temperature and its gradient in the *x* and *y* directions in the refined grid model of the Caiyuanzi iron deposit. Compared with the modeling results shown in Fig. 10, it is noted that the distributions of temperature of the refined grid model are almost the same, but more localized.

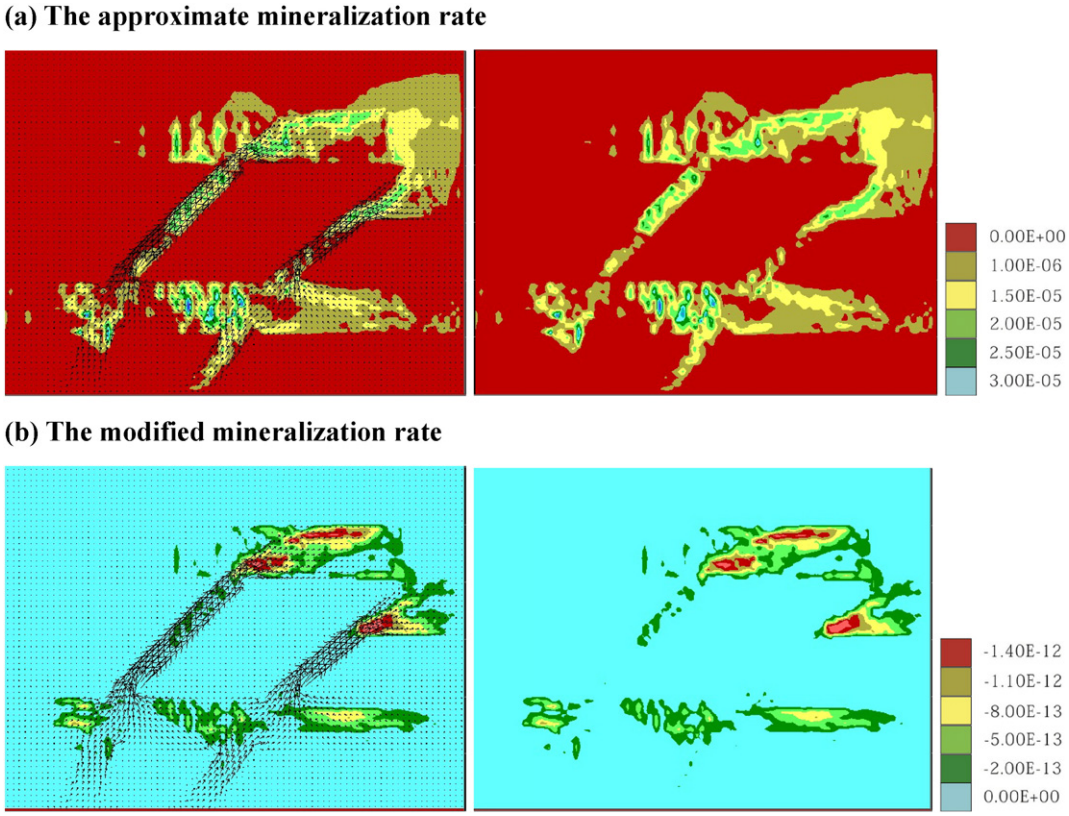

Fig. 11. Distributions of the approximate and modified mineralization rates: (a) the approximate mineralization rate and (b) the modified mineralization rate.

Fig. 14 shows the distributions of the modified mineralization rate of iron ore in the refined grid model of the Caiyuanzi iron deposit. Compared with the results shown in Fig. 11, the location of the precipitation of iron metal is the same expect for that the lower part has a little change. This indicates that the refined grid model almost has little influence on the location of the formation of the Caiyuanzi iron deposit. Thus, the numerical model used in the second example can also reflect the formation mechanism of the Caiyuanzi iron deposit, so that there is no need to use the refined grid model.

Fig. 15 shows the pore-fluid pressure and its gradients in the *x* and *y* directions in the refined grid model of the Caiyuanzi iron deposit. Obviously, these results are similar to those shown in Fig. 12, indicating that the refined grid model has little influence on the distribution of pore-fluid pressure and its gradients.

4. Discussion and conclusions

Siderite is one of the most common minerals in the Earth's crust, and easily dissolve in the hypothermal solutions. Based on this feature, the large and rich siderite ore deposits are seldom to be found, so that the Caiyuanzi iron deposit is one of the typical siderite deposits in the Guizhou province. Many factors, such as distributions of temperature, pressure, chemical components of county rock and chemical reactions of minerals, can influence the processes of the siderite mineralization. Due to the level of coding experience, only a simplified 2D model involving the coupled heat transfer and pore-fluid flow is used to produce preliminary results for investigating the possible location of the iron deposit in the Caiyuanzi ore district. As mentioned above, many previous studies believe that the siderite deposit in the Caiyuanzi ore district

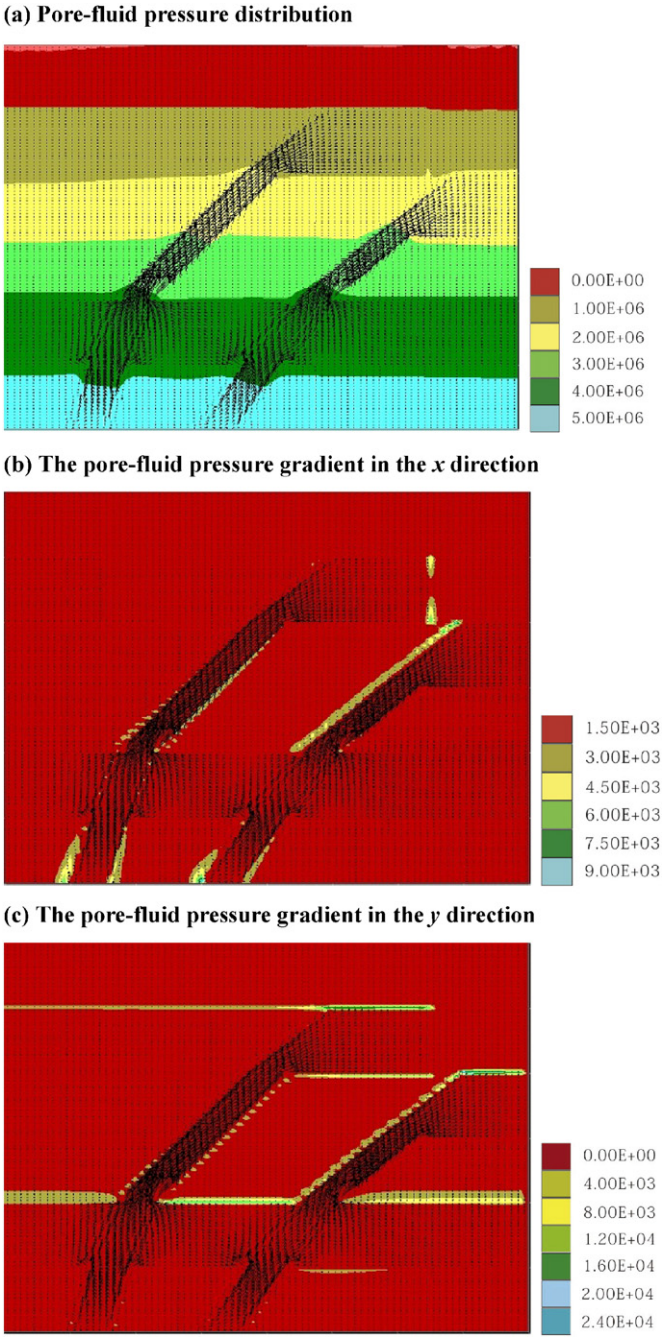

Fig. 12. Distributions of pore-fluid pressure and its gradients: (a) pore-fluid pressure distribution; (b) the pore-fluid pressure gradient in the *x* direction and (c) the pore-fluid pressure gradient in the *y* direction.

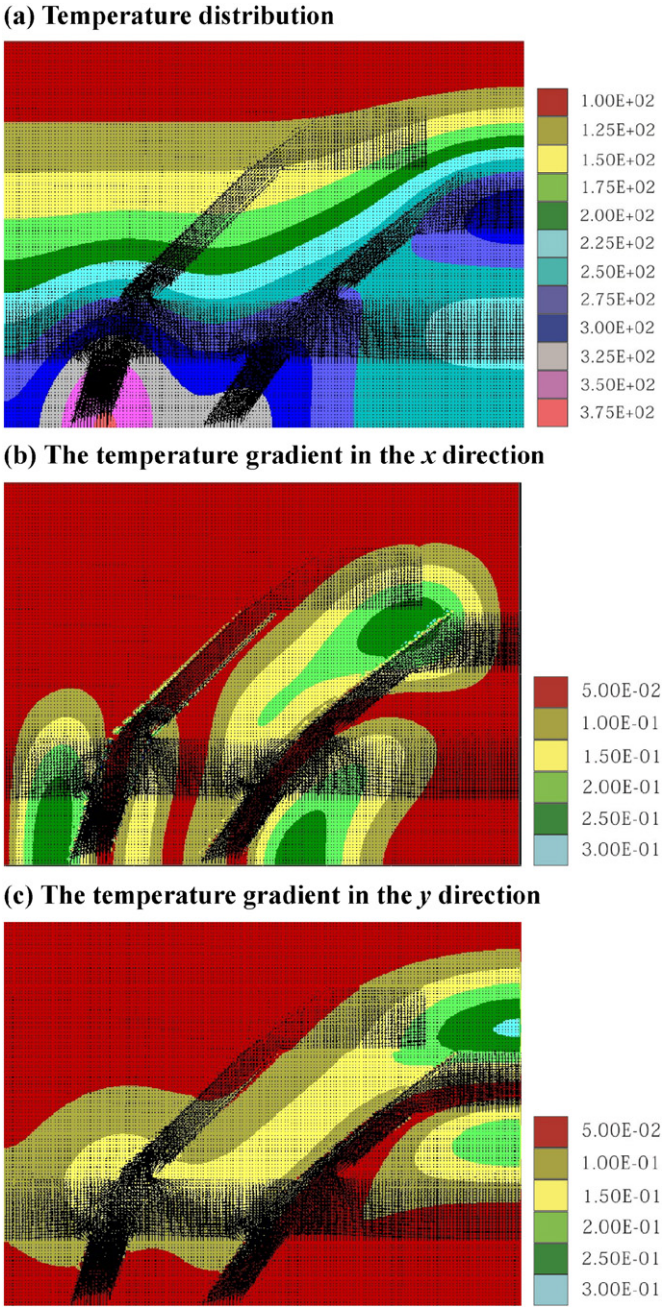

Fig. 13. Distributions of temperature and its gradients (in the case of the refined grids): (a) temperature distribution; (b) the temperature gradient in the *x* direction and (c) the temperature gradient in the *y* direction.

was formed by sedimentation, and some new studies suggest that the deposit was produced by the hydrothermal process. For this reason, this paper uses the FLAC2D program to simulate the ore-forming process of siderite in the Caiyuanzi ore deposit, so as to check whether siderite can be formed by a hydrothermal process.

Through applying the mineralization rate theory to two examples in the hydrothermal systems, the related numerical simulation results have demonstrated that:

(1) Since the rock deformation was not the controlling factor of mineralization in the Caiyuanzi ore deposit, the driving force of pore-fluid flow is the temperature gradient. The greater the temperature changes, the faster the velocity of pore-fluid flow.
(2) According to the experimental data of the chemical reaction of siderite, temperature is the core controlling factor of the chemical reaction of siderite, and the pore-fluid pressure has little effect on the precipitation of siderite. The equilibrium concentration of iron ion has changed a lot between 125 °C and 275 °C. When the ore-bearing hydrothermal solution enters the carbonate layer that provide an abundant carbonate (CO_3^{2-}), a large siderite deposit can be produced, so that iron ore-bodies are mainly located within the carbonate layer.
(3) Since the numerical results can reflect the field observations in this district basically, it has been demonstrated that the Caiyuanzi iron deposit could be formed by the hydrothermal process.

There are also some remaining problems in this study:

(1) The sedimentary process has not been considered. Many studies have shown that the siderite deposits have been produced by the sedimentary process, so that the sedimentary process is also an important factor of mineralization in the Caiyuanzi iron deposit. Due to the limitation of the computer code, the coupled hydrothermal, pore-fluid flow and sedimentary process are difficult to implement in the current computation model.
(2) The chemical reaction is simplified. In real geological systems, chemical reactions are too complicated to be confirmed precisely. However, the TOUGHREACT software (Xu et al., 2004) can be used to calculate the equilibrium concentration of iron ion (Fe^{2+}) in siderite under different temperature and pressure conditions (in the NaCl buffer). The mineralization rate is valid only when the concentration of iron ion is in the equilibrium state. However, it is known that most chemical reactions in real geological systems may be in the non-equilibrium state.
(3) The geological model is simplified. Due to the complexity of mineralization in the Caiyuanzi iron deposit, we only simulate the situation of the chemical reaction between iron ion (Fe^{2+}) and carbonate (CO_3^{2-}) without considering the influence of other ions in hydrothermal solution and county rocks. This means that the experimental data of the precipitation of siderite from TOUGHREACT is also simplified in the simulation.
(4) The geometry of the numerical model and the distribution of rock properties are much simpler than those in the real world.

It must be pointed out that the numerical model indeed has certain limitations and shortcomings. First, a numerical model should be established on the basis of the geological model, which should include the geological information as detail as possible. However, the current numerical model still cannot consider all the detailed geological information due to the existing computer capacity. Second, a numerical model can only produce approximate solutions for geological problems. To ensure the correctness of a numerical model, the numerical solutions should be validated by theoretical analyses and field observations. Nevertheless, numerical modeling has helped many geologists for solving

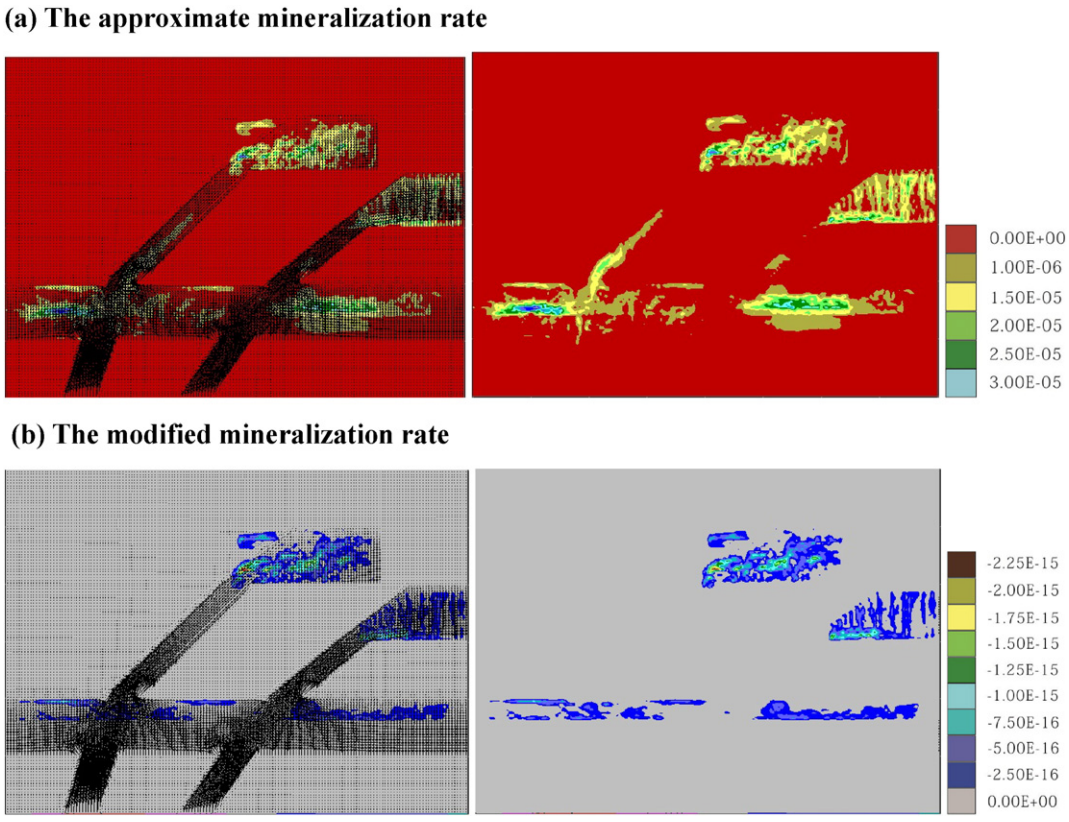

Fig. 14. Distributions of the approximate and modified mineralization rates (in the case of the refined grids): (a) The approximate mineralization rate and (b) the modified mineralization rate.

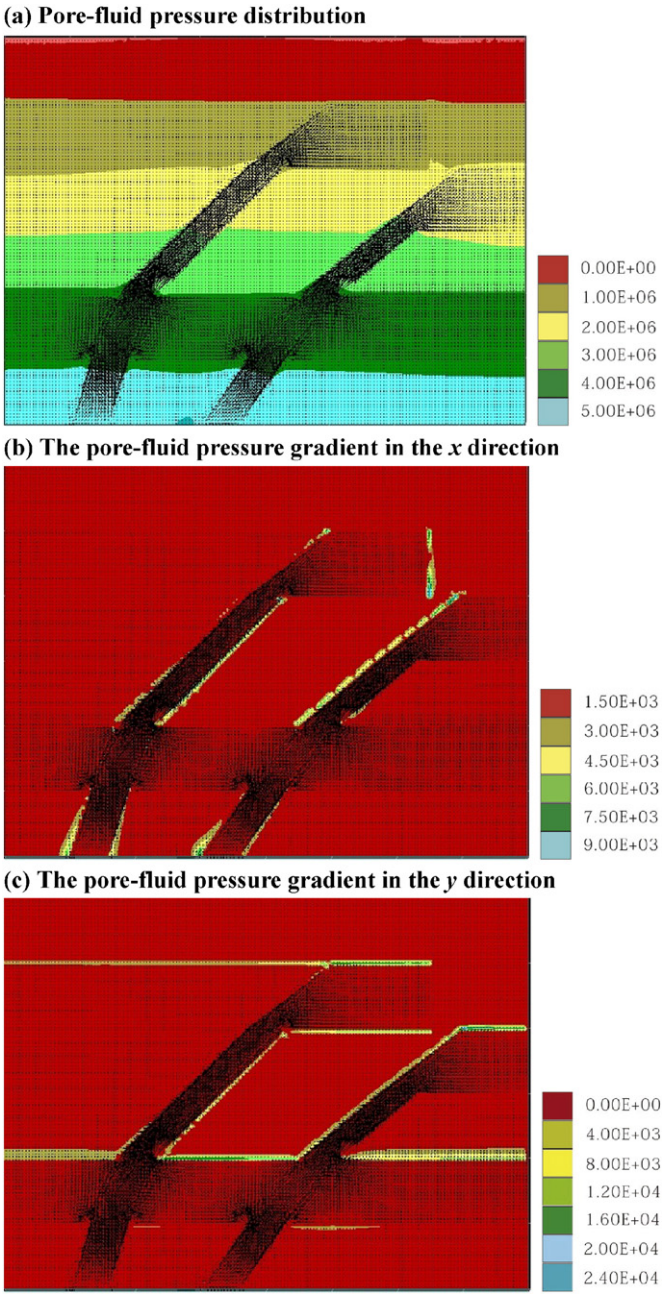

Fig. 15. Distributions of pore-fluid pressure and its gradients (in the case of the refined grids): (a) pore-fluid pressure distribution; (b) the pore-fluid pressure gradient in the *x* direction and (c) the pore-fluid pressure gradient in the *y* direction.

many complex geological problems, so that it becomes a valuable tool for investigating and exploring the processes of mineralization systems, although there are a lot of rooms for further improvement.

In this paper, the related numerical results have demonstrated that: (1) The Caiyuanzi ore deposit belongs to the epithermal iron deposit. The range of metallogenic temperature of siderite is between 125 °C and 275 °C, which is consistent with the experimental data of the ore-forming temperature in the Caiyuanzi ore district. (2) The simulation results of the modified mineralization rate can reflect the orebody location in the Caiyuanzi iron deposit, implying that the Caiyuanzi iron deposit can be formed by the hydrothermal process. (3) Simulation of coupled heat transfer and pore-fluid flow with considering the chemical reaction, to some extent, helps us to understand the process of the ore-forming of siderite in the Caiyuanzi iron deposit, and also fills the gaps of the numerical simulation research in this particular region.

Acknowledgments

The authors express their thanks to the anonymous referees for their valuable comments, which led to a significant improvement over an early version of the paper.

References

Alt-Epping, P., Zhao, B.C., 2010. Reactive mass transport modeling of a three-dimensional vertical fault zone with a finger-like convective flow regime. J. Geochem. Explor. 106, 8–23.
Cai, M., Zhan, M., Peng, S., Meng, X., Liu, G., 2002. Study of Mesozoic Metallogenic Geological Setting and Dynamic Mechanism in Yunkai Area. Mineral Deposits 21, 264–269 (in Chinese with English abstract).
Cundall, P.A., Board, M., 1988. A microcomputer program for modelling large-strain plasticity problems. In: Swoboda, C. (Ed.), Numerical Methods in Geomechanics: Proceedings, 6th International Conference on Numerical Methods in Geomechanics. Balkema, Rotterdam, pp. 2101–2108.
Forrest, P. Schumacher, Eunhye, K., 2013. Modeling the pipe umbrella roof support system in a Western US underground coal mine. Int. J. Rock Mech. Min. Sci. 60, 114–124.
Garven, G., Gee, S., Person, M.A., Sverjensky, D.A., 1993. Genesis of stratabound ore deposits in the midcontinent basins of North America. 1. The role of regional groundwater flow. Am. J. Sci. 293, 497.
Gessner, K., Kühn, M., Rath, V., Kosack, C., Blumenthal, M., Clauserss, C., 2009. Coupled process models as a tool for analysing hydrothermal systems. Surv. Geophys. 30, 133–162.
Gow, P., Upton, P., Hill, K., 2002. Copper–gold mineralization in the New Guinea: numerical modeling of collision, fluid flow and intrusion-related hydrothermal system. Aust. J. Earth Sci. 49, 753–771.
Guizhou Bureau and of Geology and Mineral Resources, 1987. Annals of Regional Geology of Zhejiang Province. Geological Publishing House, Beijing.
Hakami, H., 2001. Rock characterisation facility (RCF) shaft sinking: numerical computations using FLAC. Int. J. Rock Mech. Min. Sci. 38, 59–65.
Hobbs, B.E., Zhang, Y., Ord, A., 2000. Application of coupled deformation, fluid flow, thermal and chemical modeling to predictive mineral exploration. J. Geochem. Explor. 69, 505–509.
Hobbs, B.E., Ord, A., Peng, S., Mühlhaus, H.B., Liu, L., 2004. Theoretical investigation of convective instability in inclined and fluid-saturated three-dimensional fault zones. Tectonophysics 387, 47–64.
Hobbs, B.E., Ord, A., Kühn, M., Mühlhaus, H.B., Peng, S., 2006. Numerical simulation of double-diffusion driven convective flow and rock alteration in three-dimensional fluid-saturated geological fault zones. Comput. Methods Appl. Mech. Eng. 195, 2816–2840.
Hobbs, B.E., Ord, A., Hornby, P., Peng, S., Liu, L., 2007. Mineral precipitation associated with vertical fault zones: the interaction of solute advection, diffusion and chemical kinetics. Geofluids 7, 3–18.
Hobbs, B.E., Ord, A., Hornby, P., Peng, S., 2008. Effect of reactive surface areas associated with different particle shapes on chemical-dissolution front instability in fluid-saturated porous rocks. Transp. Porous Media 73, 75–94.
Hobbs, B.E., Ord, A., Peng, S., 2010a. Effects of mineral dissolution ratios on chemical-dissolution front instability in fluid-saturated porous rocks. Transp. Porous Media 82, 317–335.
Hobbs, B.E., Ord, A., Zhao, B.C., 2010b. Theoretical analyses of the effects of solute dispersion on chemical-dissolution front instability in fluid-saturated porous rocks. Transp. Porous Media 84, 629–653.
Hobbs, B.E., Regenauer-Lieb, K., Ord, A., 2011. Computational simulation for the morphological evolution of nonaqueous-phase-liquid dissolution fronts in two-dimensional fluid-saturated porous media. Comput. Geosci. 15, 167–183.
Hornby, P., Ord, A., Peng, S., 2006a. Numerical modelling of fluids mixing, heat transfer and non-equilibrium redox chemical reactions in fluid-saturated porous rocks. Int. J. Numer. Methods Eng. 66, 1061–1078.
Hornby, P., Peng, S., Liu, L., 2006b. Theoretical and numerical analyses of pore-fluid flow patterns around and within inclined large cracks and faults. Geophys. J. Int. 166, 970–988.
Hornby, P., Ord, A., Peng, S., Liu, L., 2008. Theoretical and numerical analyses of chemical-dissolution front instability in fluid-saturated porous rocks. Int. J. Numer. Anal. Methods Geomech. 32, 1107–1130.
Hu, J., 1985. The replacing and reforming features of siderite of Caiyuanzi in Western Guizhou. Geol. Guizhou 2, 131–134 (in Chinese with English abstract).
Itasca Consulting Group, 2002. FLAC User's Guide. Itasca Consulting Group, Inc., Minneapolis.
Ju, M., 2011. Numerical Modeling of Coupled Nonlinear Dynamic Processes of Mineralization in Dachang, Guangxi, China PhD thesis, Central South University (in Chinese with English abstract).
Ju, M., Zhao, B.C., Dai, T., Yang, J., 2011. Finite element modeling of pore-fluid flow in the Dachang ore district, Guangxi, China: implications for hydrothermal mineralization. Geosci. Front. 2 (3), 463–474.
Lei, X., Chen, Y., Zhao, J., 2013. Three-dimensional thermo-mechanical modeling of the Cenozoic uplift of the Tianshan mountains driven tectonically by the Pamir and Tarim. J. Asian Earth Sci. 62, 797–811.
Liao, S., Liang, T., Zeng, M., 1980. Discussion on mechanism of sedimentary transformation of iron ore deposits in Guizhou siderite ore beds. Geol. Rev. 26, 16–24 (in Chinese).
Lin, L., Chen, Z., Wan, H., Xu, A., Ling, Y., 1986. The characteristics of the hydrogen, oxygen and carbon isotopes and their geological signifcance of Caiyuanzi siderite deposit. Geol. Guizhou 3, 240–246 (in Chinese with English abstract).

Lin, G., Hobbs, B.E., Ord, A., Mühlhaus, H.B., 2003. Theoretical and numerical analyses of convective instability in porous media with temperature-dependent viscosity. Commun. Numer. Methods Eng. 19, 787–799.
Lin, G., Zhou, Y., Wei, X., 2006. Structure controls on fluid flow and related mineralization in the Xiangshan uranium deposit, Southern China. J. Geochem. Explor. 89, 231–234.
Lin, G., Hobbs, B.E., Zhang, L., Zhou, Y., 2008. Potential effects of upward throughflow on thermal structure models within the continental lithospheric mantle–crust. Chin. J. Geophys. 51 (2), 393–401.
Lin, G., Peng, M., Zhang, L., Zhang, D., Liu, S., 2009. Numerical analysis and simulation experiment of lithospheric thermal structures in the South China Sea and the Western Pacific. J. Earth Sci. 20, 85–94.
Liu, Y., Dai, T., 2014. Numerical modeling of pore-fluid flow and heat transfer in the Fushan iron ore district, Hebei, China: implications for hydrothermal mineralization. J. Geochem. Explor. 144, 115–127.
Liu, W., Nie, Z., 1985. Further discussion on replacing features of siderite deposit of Caiyuanzi from the result of electron probes. Geol. Guizhou 2, 137–144 (in Chinese with English abstract).
Liu, L., Yang, G., Peng, S., 2005. Numerical modelling of coupled geodynamical processes and its role in facilitating predictive ore discovery: an example from Tongling, China. Resour. Geol. 55, 21–31.
Liu, L., Zhao, Y., Zhao, B.C., 2010a. Coupled geodynamics in the formation of Cu skarn deposit in Tongling–Anqing district, China: computational modeling and implications for exploration. J. Geochem. Explor. 106, 146–155.
Liu, L., Zhou, R., Zhao, B.C., 2010b. Constraints of tectonic stress regime on mineralization system related to the hypabyssal intrusion: implication from the computational modeling experiments on the geodynamics during cooling process of the Yuenshan intrusion in Anqing district, China. Acta Petrol. Sin. 26, 2869–2878 (in Chinese with English Abstract).
Liu, L., Wan, C., Zhao, Y., 2011. Geodynamic constraints on orebody localization in the Anqing orefield, China: computational modeling and facilitating predictive exploration of deep deposits. Ore Geol. Rev. 43, 249–263.
Nie, Z., 1986. The mineralogical study of siderite of the Caiyuanzi siderite deposit. Geol. Guizhou 4, 341–355 (in Chinese with English abstract).
Ohmoto, H., Lasage, A., 1982. Kinetics of reactions between aqueous sulfates and sulfides in hydrothermal systems. Geochim. Cosmochim. Acta 46, 1727–1745.
Ord, A., Hobbs, B.E., Zhang, Y., Broadbent, G.C., Brown, M., Willetts, G., Sorjonen-Ward, P., Walshe, J., 2002. Geodynamic modeling of the Century deposit, Mt Isa Province, Queensland. Aust. J. Earth Sci. 49, 1011–1039.
Ord, A., Hornby, P., Peng, S., 2008a. Morphological evolution of three-dimensional chemical dissolution front in fluid-saturated porous media: a numerical simulation approach. Geofluids 8, 113–127.
Ord, A., Peng, S., Liu, L., 2008b. Inversely-mapped analytical solutions for flow patterns around and within inclined elliptic inclusions in fluid-saturated rocks. Math. Geosci. 40, 179–197.
Ord, A., Hobbs, E.B., Zhao, B.C., 2010. Theoretical and numerical investigation into roles of geofluid flow in ore forming systems: integrated mass conservation and generic model approach. J. Geochem. Explor. 106, 251–260.
Ord, A., Hobbs, E.B., Zhao, B.C., 2012. Effects of domain shapes on the morphological evolution of nonaqueous-phase-liquid dissolution fronts in fluid-saturated porous media. J. Contam. Hydrol. 138–139, 123–140.
Ord, A., Hobbs, E.B., Zhao, B.C., 2013a. Analytical solutions of nonaqueous-phase-liquid dissolution problems associated with radial flow in fluid-saturated porous media. J. Hydrol. 494, 96–106 2013.
Ord, A., Hobbs, E.B., Zhao, B.C., 2013b. Effects of medium permeability anisotropy on chemical-dissolution front instability in fluid-saturated porous rocks. Transp. Porous Media 99, 119–143.
Pauling, L., 1988. General Chemistry. Dover Publications Inc., New York.
Peng, S., Ord, A., Hobbs, B.E., Zhao, B.C., 2008. Particle simulation of spontaneous crack generation associated with the laccolithic type of magma intrusion processes. Int. J. Numer. Methods Eng. 75, 1172–1193.
Peng, S., Liu, L., Ord, A., 2011. Computational simulation of convective flow in the Earth's crust with consideration of dynamic crust–mantle interactions. J. Cent. S. Univ. Technol. 18, 2080–2084.
Phillips, O.M., 1991. Flow and Reactions in Permeable Rocks. Cambridge University Press, Cambridge.
Poulet, T., Regenauer-Lieb, K., 2015a. Numerical modeling of toxic nonaqueous-phase-liquid removal from contaminated groundwater systems: mesh effect and discretization error estimation. Int. J. Numer. Anal. Methods Geomech. 39, 571–593.
Poulet, T., Regenauer-Lieb, K., 2015b. Replacement of annular domain with trapezoidal domain in computational modeling of nonaqueous-phase-liquid dissolution-front propagation problems. J. Cent. South Univ. 22, 1841–1846.
Poulet, T., Regenauer-Lieb, K., Hobbs, B.E., 2013. Computational modeling of moving interfaces between fluid and porous medium domains. Comput. Geosci. 17, 151–166.
Reid, L.B., Regenauer-Lieb, K., Poulet, T., 2012a. A porosity-gradient replacement approach for computational simulation of chemical-dissolution front propagation in fluid-saturated porous media including pore-fluid compressibility. Comput. Geosci. 16, 735–755.
Reid, L.B., Regenauer-Lieb, K., Zhao, B.C., 2012b. Some fundamental issues in computational hydrodynamics of mineralization. J. Geochem. Explor. 112, 21–34.
Schaubs, P., Zhao, B.C., 2002. Numerical modelling of gold-deposit formation in the Bendigo–Ballarat zone, Victoria. Aust. J. Earth Sci. 49, 1077–1096.
Schmidt Mumm, A., Brugger, J., Schacht, U., 2010. Fluids in geological processes: the present state and future outlook. J. Geochem. Explor. 106, 1–7.
Sorjonen-Ward, P., Zhang, Y., 2002. Numerical modelling of orogenic processes and mineralization in the south eastern part of the Yilgarn Craton, Western Australia. Aust. J. Earth Sci. 49, 935–964.
Strayer, L.M., Hudleston, P.J., Lorig, L.J., 2001. A numerical model of deformation and fluid-flow in an evolving thrust wedge. Tectonophysics 335, 121–145.
Tiziana, A., Claudia, C., Andrea, M., Alessandro, T., 2013. Understanding Etna flank instability through numerical models. J. Volcanol. Geotherm. Res. 251, 112–126.
Turcotte, D.L., Schubert, G., 2002. Geodynamics. Cambridge University Press, Cambridge.
Walshe, J.L., Mühlhaus, H.B., Ord, A., 2001. Finite element modelling of fluid–rock interaction problems in pore-fluid saturated hydrothermal/sedimentary basins. Comput. Methods Appl. Mech. Eng. 190, 2277–2293.
Xiao, H., He, X., Feng, T., Wang, E., 2005. Research on coupling laws between EME and stress fields during deformation and fracture of mine tunnel excavation based on FLAC2D. Chin. J. Rock Mech. Eng. 24, 2304–2309 (in Chinese with English abstract).
Xie, H., Zhou, H., Wang, J., Li, L., Kwasniewski, M.A., 1999. Application of FLAC to predict ground surface displacements due to coal extraction and its comparative analysis. Chin. J. Rock Mech. Eng. 18, 397–401 (in Chinese with English abstract).
Xing, H.L., Makinouchi, A., 2008. Three-dimensional finite element simulation of large-scale nonlinear contact friction problems in deformable rocks. J. Geophys. Eng. 5, 27–36.
Xu, T., Sonnenthal, E., Spycher, N., Pruess, K., 2004. TOUGHREACT user's guide: a simulation program for nonisothermal multiphase reactive geochemical transport in variably saturated geologic media. Earth Sciences Division, Lawrence Berkeley National Laboratory Report CA 94720, Berkeley, California.
Yan, Y., Lin, G., Wang, Y.J., Guo, F., 2003. Apatite fission track age of Mesozoic sandstones from Beipiao basin, eastern China: implications for basin provenance and tectonic evolution. Geochem. J. 37, 377–389.
Yan, Y., Tao, P., Liu, R., 2012. REE geochemical study of Caiyuanzi iron deposit in Hezhang, Guizhou. Guizhou Geol. 29, 145–150 (in Chinese with English abstract).
Yang, J.W., Feng, Z., Luo, X., Chen, Y., 2010. Three-dimensional numerical modeling of salinity variations in driving basin-scale ore-forming fluid flow: example from Mount Isa Basin, northern Australia. J. Geochem. Explor. 106, 236–243.
Yang, R., Yuan, S., Wei, H., Chen, J., Cheng, M., 2011. Sediment geochemical character of carboniferous "Qingzhen-type Fe deposit" in central Guizhou area. Geol. Rev. 57, 24–34 (in Chinese with English abstract).
Zhai, M., 2008. Lower crust and lithospheric mantle beneath the North China Craton before the Mesozoic lithospheric disruption. Acta Petrol. Sin. 24, 2185–2204 (in Chinese with English abstract).
Zhang, Y., Barnicoat, A., Lin, G., 2003. The influence of faulting on host-rock permeability, fluid flow and ore genesis of gold deposits: a theoretical 2D numerical model. J. Geochem. Explor. 78–79, 279–284.
Zhang, Y., Schaubs, P.M., Barnicoat, A., 2008. Fault-related dilation, permeability enhancement, fluid flow and mineral precipitation patterns: numerical models. In: Wibberley, C.A.J., Kurz, W., Imber, J., Holdsworth, R.E., Collettini, C. (Eds.), The Internal Structure of Fault Zones: Implications for Mechanical and Fluid-flow Properties. Geol. Soc. Spec. Pub. 299, pp. 239–255 (London).
Zhang, L., Li, Z., Lin, G., Guo, H., 2011. Numerical simulation of effects of upward throughflow on thermal structure and the thickness of the continental lithosphere. J. Geophys. Eng. 8, 322–329.
Zhang, J., Yang, J., Yang, X., He, T., 2014. Geological characteristics and prospecting potential of sub-siderite deposit in Hezhang, Guizhou. Geol. Chem. Miner. 36, 24–30 (in Chinese with English abstract).
Zhao, C., 2009. Dynamic and Transient Infinite Elements: Theory and Geophysical, Geotechnical and Geoenvironmental Applications. Springer, Berlin.
Zhao, C., 2014. Physical and Chemical Dissolution Front Instability in Porous Media: Theoretical Analyses and Computational Simulations. Springer, Berlin.
Zhao, C., 2015. Advances in numerical algorithms and methods in computational geosciences with modeling characteristics of multiple physical and chemical processes. Sci. China Technol. Sci. 58, 783–795.
Zhao, C., Hobbs, B.E., Mühlhaus, H.B., 1998. Finite element modelling of temperature gradient driven rock alteration and mineralization in porous rock masses. Comput. Methods Appl. Mech. Eng. 165, 175–187.
Zhao, C., Lin, G., Wang, Y., Mühlhaus, H.B., Ord, A., 2002. Finite element modeling of reactive fluids mixing and mineralization in pore-fluid saturated hydrothermal/sedimentary basins. Eng. Comput. 19, 364–385.
Zhao, C., Hobbs, B.E., Ord, A., 2008a. Convective and Advective Heat Transfer in Geological Systems. Springer, Berlin.
Zhao, C., Hobbs, B.E., Ord, A., 2008b. Investigating dynamic mechanisms of geological phenomena using methodology of computational geosciences: an example of equal-distant mineralization in a fault. Sci. China Ser. D Earth Sci. 51, 947–954.
Zhao, C., Hobbs, B.E., Ord, A., 2009. Fundamentals of Computational Geoscience: Numerical Methods and Algorithms. Springer, Berlin.
Zhao, C., Hobbs, B.E., Ord, A., 2010. Theoretical analyses of nonaqueous-phase-liquid dissolution induced instability in two-dimensional fluid-saturated porous media. Int. J. Numer. Anal. Methods Geomech. 34, 1767–1796.
Zhao, C., Hobbs, B.E., Ord, A., 2012. Effects of medium and pore-fluid compressibility on chemical-dissolution front instability in fluid-saturated porous media. Int. J. Numer. Anal. Methods Geomech. 36, 1077–1100.
Zhao, C., Hobbs, B.E., Ord, A., 2013. Theoretical analyses of acidization-dissolution front instability in fluid-saturated carbonate rocks. Int. J. Numer. Anal. Methods Geomech. 37, 2084–2105.
Zhao, C., Hobbs, B.E., Alt-Epping, P., 2014. Modelling of ore-forming and geoenvironmental systems: roles of fluid flow and chemical reaction processes. J. Geochem. Explor. 144, 3–11.
Zhao, C., Hobbs, B.E., Ord, A., 2015a. Theoretical analyses of chemical dissolution-front instability in fluid-saturated porous media under non-isothermal conditions. Int. J. Numer. Anal. Methods Geomech. 39, 799–820.
Zhao, C., Hobbs, B.E., Ord, A., 2015b. Computational simulation of chemical dissolution-front instability in fluid-saturated porous media under non-isothermal conditions. Int. J. Numer. Methods Eng. 102, 135–156.